

**Analysis of Microgrid Stability and dynamic simulation of Dependent Source Model by using PSO**S.AnandaKumar¹, M.Kumudwathi²¹M.Tech, Electrical and Electronics Engineering, Sri Krishnadevaraya University college of Engineering And Technology, Ananthapuramu, A.P, India²Lecturer, Electrical and Electronics Engineering, Sri Krishnadevaraya University college of Engineering And Technology, Ananthapuramu, A.P, India

Abstract — The power systems are responsible for energy transportation in the form of electricity, are subjected to a number of disturbances such as frequency variation or voltage fluctuation. These may impact to the devices which we are connected to the network. An effective storage system such as battery energy storage systems (BESS) may bring the network many advantageous. There are several models to examine the BESS for micro grid stability analysis such as detailed model, ideal dc link model, and an average model. All the models share the same parameters and the control strategy. In this paper a Dependent Source Model (DSM) is proposed for modeling the battery energy storage system (BESS) for micro grid stability. Here in the proposed model, switches are replaced by dependent voltage and current sources and the control system remains the same. To obtain optimum PI controller settings for a non-linear process a Particle Swarm Optimization (PSO) technique is used. In this paper optimum values of PI controller settings are found and it is proved that the PSO based tuned PI values in the DSM model gives better results than the gain scheduling methods.

Keywords- Battery Energy Storage System (BESS), Micro grid, Dependent Source Model (DSM), PSO, Stability.

I. INTRODUCTION

The electric system became the basis of modern society, without any prospect of slowing down. The Micro Grid concept assumes a cluster of loads and micro sources operating as a single controllable system, interconnected by a small electrical grid of medium or low voltage. The micro-grid is scaled with the purpose of owning enough resources to supply the connected customers, and it is regarded by the electrical grid upstream as a single customer. Nevertheless, the network keeps on being fragile, subject to a number of disturbances such as fluctuations in frequency or voltage variations.

However, such active distribution networks present various challenges, such as the integration of plug-in electric vehicles and the proliferation of renewable energy sources (RES), which have to be addressed when significant penetration levels are reached. In this context, BESS can be practically helpful to deal with such challenges, as explained next.

In order to take full advantage of renewable energies and mitigate their problems, such as the variability and intermittency of the resources that influence the stability of the grid, it is advisable to implement an energy storage system such as the BESS.

For several interesting technical features, BESS have received considerable attention recently, particularly as a solution to the challenges facing modern active distribution networks and micro-grids. BESS can provide several key ancillary services, such as load shifting, dynamic local voltage support, short-term frequency smoothing, grid contingency support, and reduce the need for fossil-fuel-based generation. Therefore, BESS are considered a key enabling element of modern smart grids and micro-grids.

In the proposed where the switches are replaced by dependent sources and the control system remains the same to help analyzing the differences observed in the performance of the models. The models are developed in MATLAB and their performances are compared by considering various variables such as voltages and currents at the point-of-common-coupling, active and reactive power injection, and total harmonic distortion, in the context of the impact on the stability of the system. To obtain optimum PI controller settings for a non-linear process a Particle Swarm Optimization (PSO) technique is used in the proposed model. The main objectives and contributions of the paper are the following:

1. Develop and study various BESS models for micro grid simulation and analysis, including a new and efficient model of DSM where the switches are replaced by dependent sources, identifying the conditions in which each model can be used. A PSO algorithm is used to tune the PI controller is applied to isolate and evaluate the impact of various parameters in the network.
2. Study the impact of BESS dc link voltage dynamics on micro grid stability through the tuned values of PI controller.
3. Study and demonstrate the impact of unbalanced loading on micro grids stability.

4. Compare the performance of the proposed models in a realistic test micro grid, determining their advantages and limitations, and their computational efficiency.

II. BESS MODEL

The BESS models used in this paper mainly include a buck/boost converter, a dc link capacitor, a three-phase bidirectional dc-ac converter, an ac filter, and a transformer connecting the system to the micro grid. In this section, these models and the corresponding parameters are discussed, and the control techniques used for each BESS converter are also described. Figure 8 depicts in detail the BESS components [5].

A. Battery

The battery model described here is based on the generic model proposed in [13], and is modeled as a controllable ideal dc source in series with an internal resistance R_B . The no-load voltage of the battery E_B is calculated based on the state-of-charge (SOC) of the battery using a nonlinear equation, as follows:

$$E_B = E_0 - K \frac{1}{SOC} + A^{-BQ(1-SOC)} \quad (1)$$

Where E_0 is the battery constant voltage in V, K is the polarization voltage in V, Q is the battery capacity in Ah, and A and B are parameters determining the charge/discharge characteristics of the battery. The parameters A, B and K can be tuned to mimic a specific battery type discharge characteristic. Note that the time frame of the test scenarios discussed in this paper is in the order of a few seconds; hence, since the BESS designed and simulated in this paper has a rated power of 1 MW and a rated capacity of 1 MWh, which is a typical power to capacity ratio for BESS in micro grids, the battery voltage and SOC relation cannot be observed in the presented simulation results.

B. Buck/Boost Converter

The buck/boost converter is in charge of controlling the dc link capacitor voltage by properly charging and discharging the battery. A cascaded PI controller is used here to generate the duty cycle for the switches based on the difference of the dc link voltage and its set-point, as shown in Fig. 2. Note that the second PI controller reacts to changes in the active power of the system first, thus improving the ability of the buck/boost controller to maintain the dc link voltage. When the dc link voltage is lower than the pre-defined set-point, the converter works in the boost mode, discharging the battery. When the dc link voltage is higher than the set point, the converter operates in the buck mode, charging the battery. The current ripple is bounded by a proper choice of the inductor L chop f , as follows [14]:

$$\Delta I = \frac{E_B}{I_{chopf}} \Delta t = \frac{E_B}{I_{chopf}} \frac{1}{2f_s} \quad (2)$$

Where f_s is the switching frequency.

C. DC-AC Converter

Figure 8 illustrates how the dc-ac converter connects the battery and buck/boost converter to the grid through the ac filter. The converter control system provides the voltage magnitude and phase set-points to create sinusoidal reference signals for the Pulse Width Modulation (PWM) scheme of the converter. As shown in Fig. 8, when the switches are in State 1, the voltage magnitude and phase set-points are obtained based on the reference voltage and frequency; thus, the BESS in this case is the master voltage and frequency controller of the system, which is referred to as a grid-forming control technique. If the switches are in State 2, the voltage magnitude and phase set-points are obtained based on the reference active and reactive powers; hence, the battery is operated in constant PQ mode, injecting/absorbing constant active and reactive power, which is referred to as grid-feeding mode. Grid supporting and grid-following control modes are based on these two fundamental control strategies, and are accomplished by changing the reference voltage, frequency, active power, and/or reactive power [15]. Observe that these controls are based on Park's dq-axes transformations.

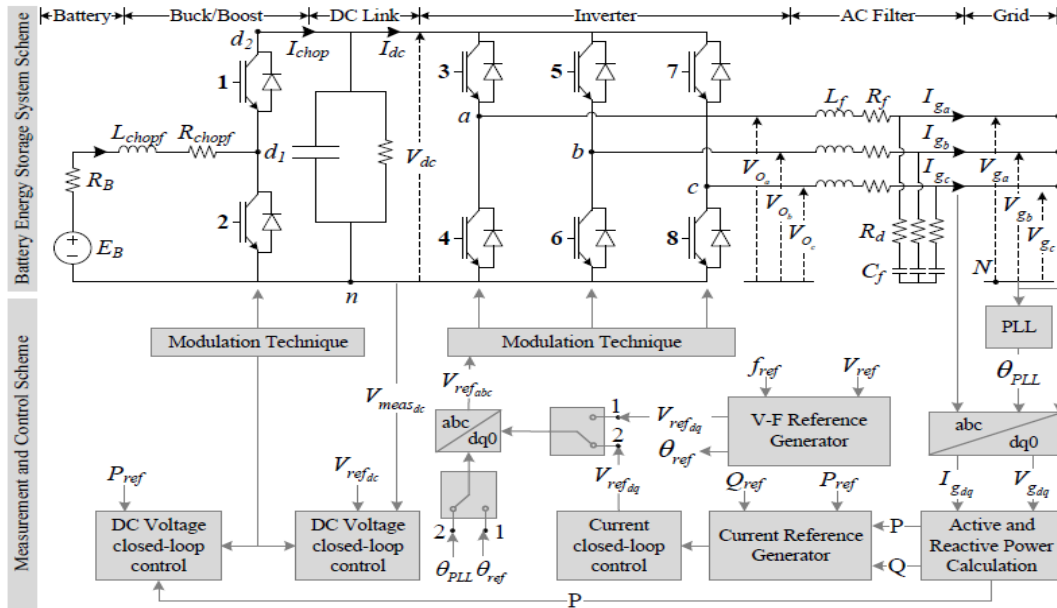


Fig1. schematic of battery energy storage system components and its controls

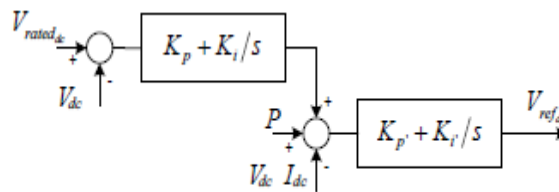


Fig.2. Buck boost Dc link voltage controller

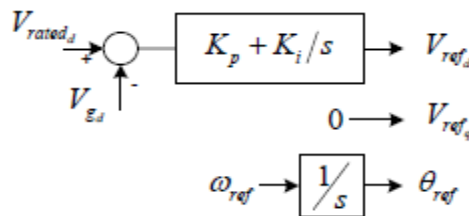


Fig.3. Grid forming voltage and phase reference generator

In the grid-forming mode, the voltage dq-axes reference set-points would be directly used to create the abc-reference signals, as shown in Fig. 3. The reference angle is obtained by integrating the reference angular frequency. Observe that a PI controller is used to maintain the point of common coupling (PCC) voltage at its rated value. In grid-feeding control mode, the injected active and reactive power are calculated first, as follows:

$$P = \frac{3}{2} (V_{gd} I_{gd} - V_{gq} I_{gq}) \quad (3)$$

$$q = \frac{3}{2} (V_{gd} I_{gq} - V_{gq} I_{gd}) \quad (4)$$

To obtain the corresponding fundamental P and Q components, the instantaneous active p and reactive q powers are passed through low-pass filters. The fundamental active and reactive powers are then passed through the current reference generator block to obtain the current dq-axes reference set points, as follows:

$$I_{refd} = \frac{3}{2} \frac{P_{ref} V_{gd} + Q_{ref} V_{gq}}{V_{gd}^2 + V_{gq}^2} \quad (5)$$

$$I_{refq} = \frac{3}{2} \frac{P_{ref} V_{gq} + Q_{ref} V_{gd}}{V_{gd}^2 + V_{gq}^2} \quad (6)$$

These current references are then passed through the current closed-loop control to obtain the final voltage dq-axes references; feed-forward terms should be used to decouple the two axes, and should be considered for the difference between the voltages after and before the ac filter. Neglecting R_d , a single line diagram can be used to derive such a relation, as shown in Fig. 4, resulting in the following equations:

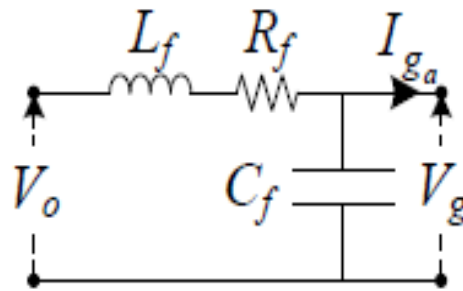


Fig.4. Single line diagram of ac filter

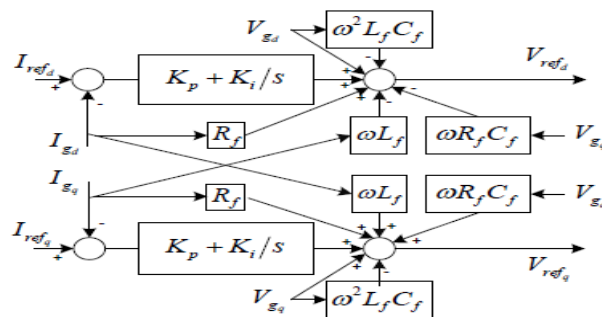


Fig.5. Current closed-loop control

$$V_{od} = V_{gd} (1 - \omega^2 L_f C_f) + I_{gd} R_f - I_{gq} \omega L_f - V_{gq} \omega R_f C_f \quad (7)$$

$$V_{oq} = V_{gq} (1 - \omega^2 L_f C_f) + I_{gd} R_f + I_{gd} \omega L_f + V_{gd} \omega R_f C_f \quad (8)$$

The final current closed-loop control block shown in Fig. 5 can be obtained from these equations. The output of the current controller are the voltage references V_{refd} and V_{refq} , which are transformed back to the abc-reference frame to obtain the sinusoidal control signals for PWM scheme of the converter. More information on alternative converter controls such as grid-supporting and grid following can be found in [15].

D. AC Filter:

The ac filter should be designed properly to limit output current ripple and achieve an acceptable damping rate. The ac filter inductor L_f in a dc-ac converter can be determined based on the maximum acceptable current ripple, the dc link voltage, and the switching frequency as follows [16]:

$$\Delta I_{max} = \frac{V_{dc}/3}{L_f 4f_s} \quad (9)$$

The ac filter capacitor C_f reactive power injection has to be less than 5% of the converter rated power [16]. A series damping resistance is considered to prevent harmonic oscillations, and is assumed to consume 0.2% of the rated power as per:

$$R_d = \frac{V_f^2}{0.002P_f} - \sqrt{\left(\frac{V_f^2}{0.002P_f}\right)^2 - \frac{1}{(\omega C_f)^2}} \quad (10)$$

Also, a resistance R_f is added in series with the filter inductance to represent its parasitic resistance losses.

III. ESS APPROXIMATE MODELS

In the previous section, the different BESS components and their corresponding controls are discussed in detail. Models have been proposed in the literature, in which some components of the detailed BESS model are eliminated to achieve faster simulation speed and/or reduce control complexity, as explained next.

A. Ideal DC Link Model:

The schematic of this model is shown in Fig. 6, where the battery model along with the buck-boost converter is replaced by an ideal dc source, thus fixing the dc link voltage. Hence, the controls related to the dc link are eliminated. The rest of the system remains the same, i.e. the inverter and the ac filter and the corresponding control are the same as explained in Section II.

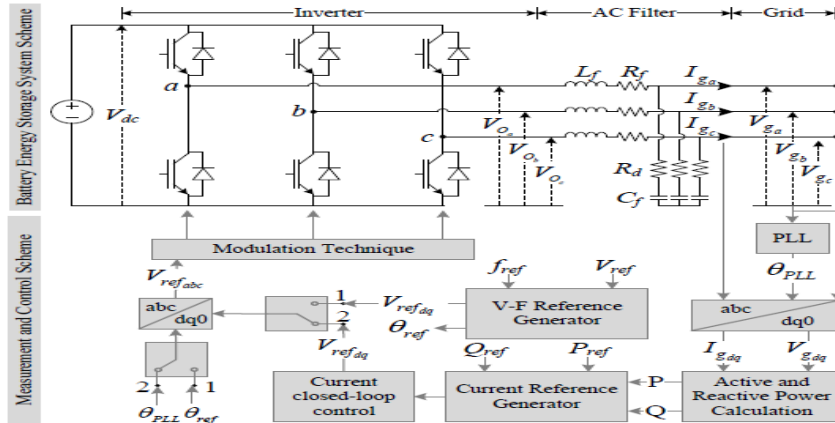


Fig.6. Ideal dc link model of the BESS

B. Average Model:

The schematic of this model is shown Fig. 7, where the entire switching system is replaced by ideal voltage sources, i.e. the battery, buck-boost converter, and dc-ac inverter are eliminated; this increases the simulation speed significantly. The control system for the battery remains the same as in Section II; the only change is that abc-reference signals are directly fed to the ideal voltage sources, and the PWM scheme controls are eliminated.

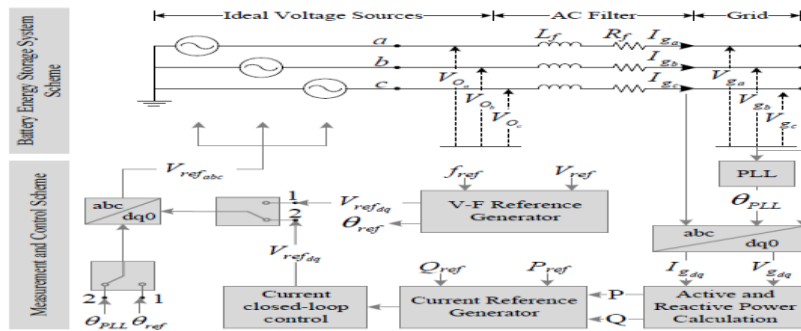


Fig.7. Average model of the BESS

C. Dependent Source Model (DSM):

To identify and isolate the impact of switches on the performance of the system, a model is proposed here in which the switches are replaced by dependent voltage and current sources, as shown in Fig. 8. The control system remains the same as in Fig. 1. Two models are developed based on the value of the dependent voltage and current sources, as explained next.

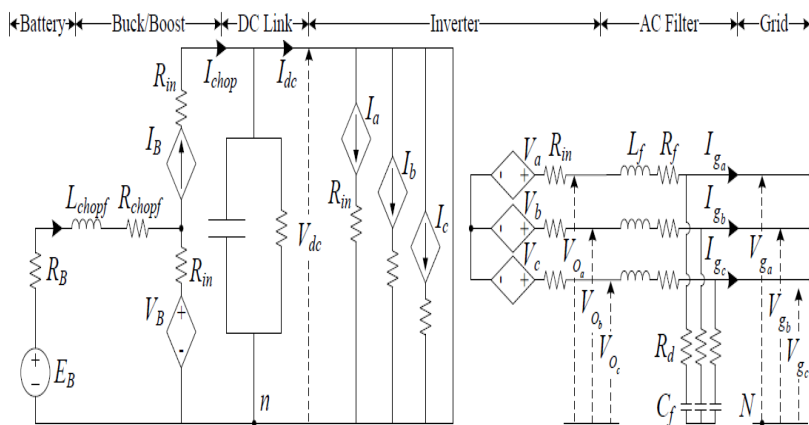


Fig.8. Schematic of a battery energy storage system with switches being replaced by dependent sources

IV. Simulation Results

To effectively compare the performance of the three different modeling approaches, a test system based on the CIGRE benchmark for medium voltage distribution network is implemented in PSCAD/EMTDC, as shown in Fig. 9. The test system has a 1.3 MVA diesel-based synchronous machine, a 1 MW BESS, and a 1 MW wind turbine, with the latter

being modeled using an average model similar to Fig. 7, and operated as a constant power source for the short duration of time it is connected to the grid, since the disconnection of the wind turbine is used here as a disturbance. The diesel-based synchronous machine and its exciter and governor are tuned and validated according the actual measurements from a commercial grade synchronous machine. The loads are modeled using a voltage-sensitive exponential model with a 1.5 exponent, which is a reasonable value for typical isolated microgrids. The load demand and unbalance levels are different for each test scenario discussed next.

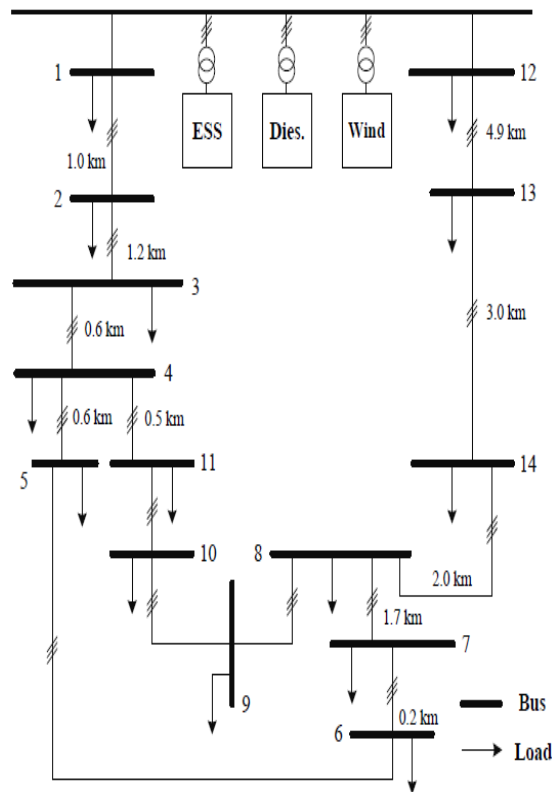


Fig.9. Modified version of CIGRE benchmark microgrid

In the detailed model the energy storage system obtained the performance different cases. Such as grid forming BESS based in balanced operation, grid forming BESS based in unbalanced operation, grid forming BESS with wind generator outage, grid supporting BESS with wind generator outage. The results above conditions shown below.

A. Particle swarm optimization:

Initialize the population of particles with random position and velocities in the dimensional problem space. Confine the search space by specifying the lower and upper limits of each decision variable. The population points are initialized with the velocity and position set to fall into the pre-specified or allowed range and to satisfy the equality and inequality constraints.

PSO algorithm consists of the following steps like initialization, velocity updating, position updating, and memory updating termination criteria examination.

Optimal Parameters of PSO: For all the problems considered the following parameters give optimal results:

- Population Size
 - Acceleration coefficients (c1, c2)
 - w is varied from 1.4 to 0.4
- Maximum velocity V_{max} is limited to 10% of the dynamic range of the variables on each dimension.

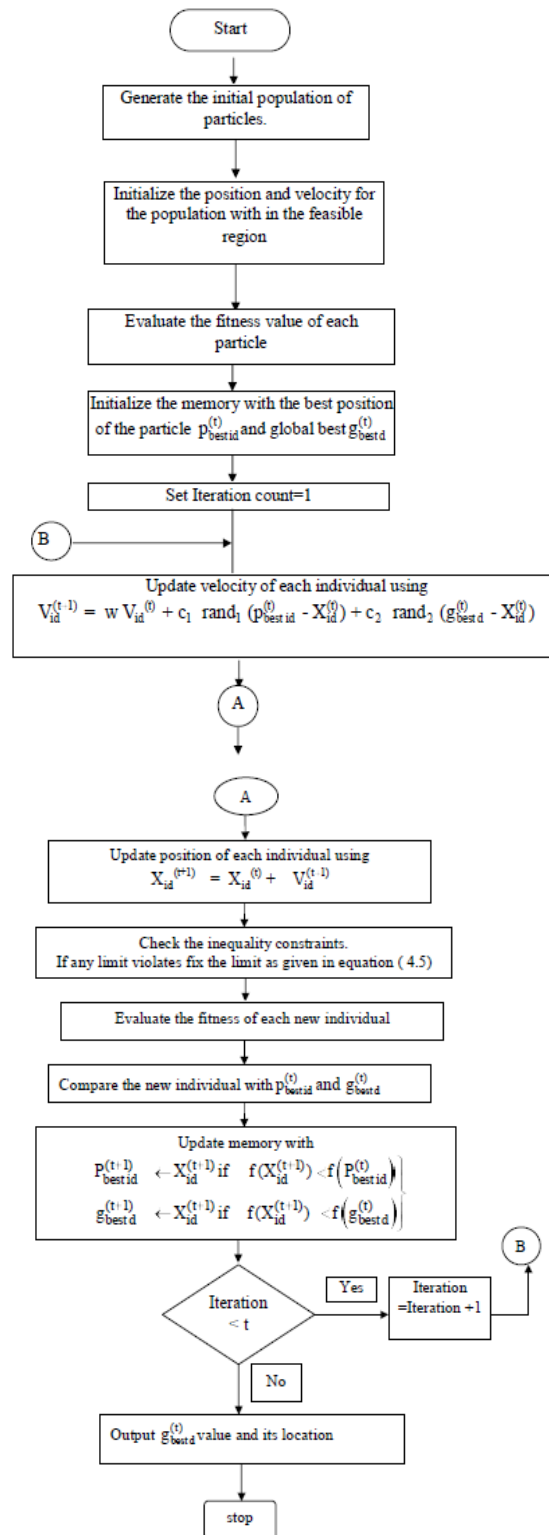


Table.1. PSO algorithm

B. Grid forming BESS based in balanced operation:

In this case, the diesel and wind generators are not connected. The system load is 950 kW of active power and 100kVar of reactive power, balanced among the three phases; at t = 0:5s, the load is increased by 100kVar, and at t = 11:5s, the reactive power load is again increased by 100kVar; note that the active power load is near the BESS rated power.

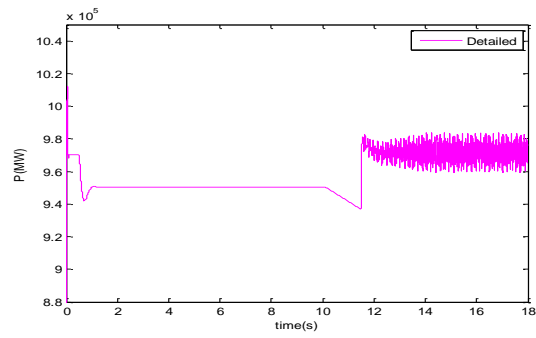


Fig.10. Detailed active power at balanced condition

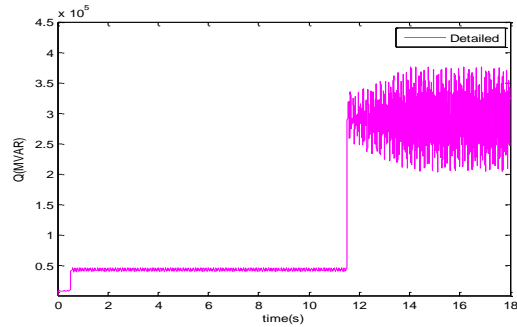


Fig.11. Detailed reactive at balanced condition

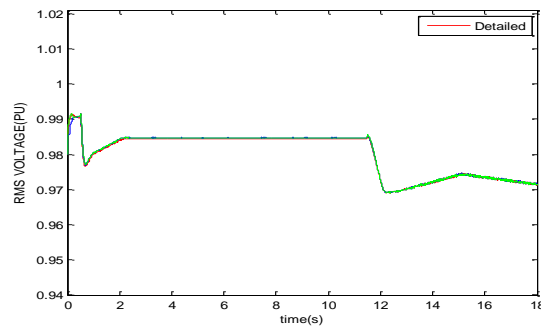


Fig.12. Detailed RMS Voltage at balanced condition

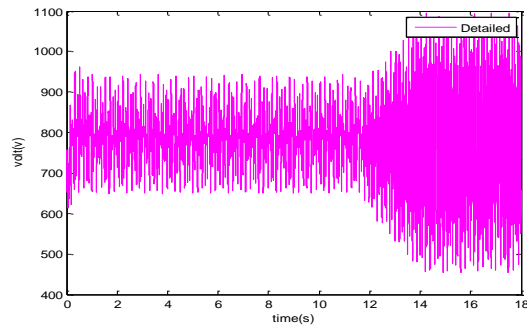


Fig.13. Detailed dc link voltage at balanced condition

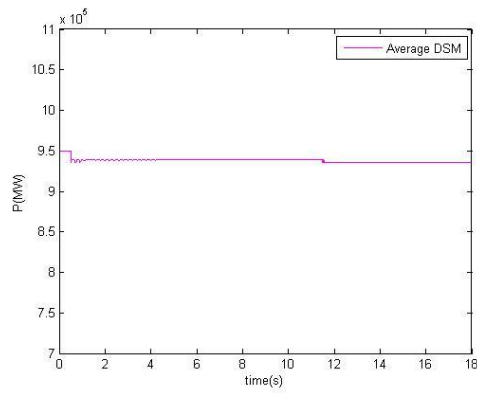


Fig.14. DSM active power at balanced condition

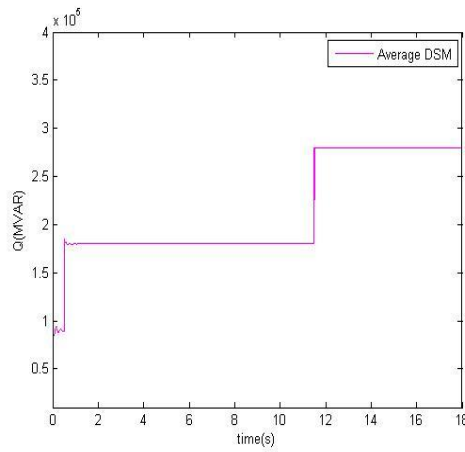


Fig.15. DSM reactive power at balanced condition

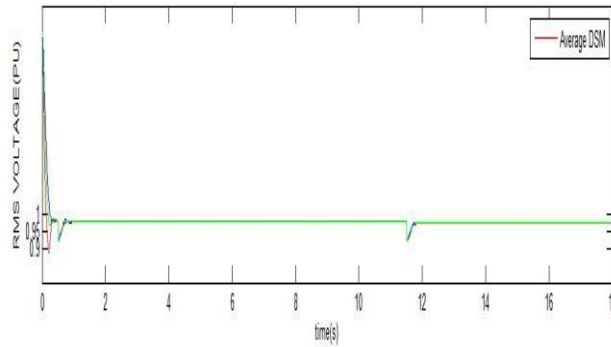


Fig.17. DSM RMS Voltage at balanced condition

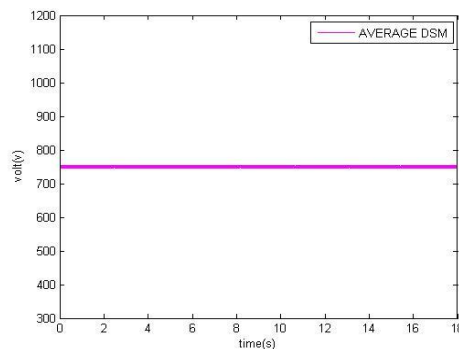


Fig.18. DSM DC Link Voltage at balanced condition

V. Conclusion

In this paper Dependent Source Model that included all necessary modeling and control details. The performance of battery energy storage system at different conditions by using particle swarm optimization discussed in this paper. This paper mainly aim to control the active power and reactive power while changing the load at different condition suddenly, The loads are considering as balanced loads. While changing the loads determine the performance of battery energy storage system discussed in this project. Several conditions applied like changing the load or increasing suddenly at specific time observing the performance of battery energy storage system. The energy storage system classified several types depends upon way of connection. The performance of energy storage system by using Particle swarm optimization algorithm obtained in the Mat Lab.

VI. References

1. Lasseter RH, Eto JH, Schenkman B, Stevens J, Vollkommer H, Klapp D, Linton E, Hurtado H, Roy J. CERTS microgrid laboratory test bed. *IEEE Transactions on Power Delivery*. 2010 Dec 23;26(1):325-32.
2. Basso T, DeBlasio R. IEEE smart grid series of standards IEEE 2030 (interoperability) and IEEE 1547 (interconnection) status. National Renewable Energy Lab.(NREL), Golden, CO (United States); 2012 Apr 1.
3. Guerrero JM, Blaabjerg F, Zhelev T, Hemmes K, Monmasson E, Jemei S, Comech MP, Granadino R, Frau JI. Distributed generation: Toward a new energy paradigm. *IEEE Industrial Electronics Magazine*. 2010 Mar;4(1):52-64.
4. Tuyen, Nguyen Duc, et al. "Analysis of transient-to-island mode of power electronic interface with conventional dq-current controller and proposed droop-based controller." *Electrical Engineering* 99.1 (2017): 47-57.
5. Delille, Gauthier, et al. "Energy storage systems in distribution grids: New assets to upgrade distribution network abilities." *CIREN 2009-20th International Conference and Exhibition on Electricity Distribution-Part 1*. IET, 2009
6. Delille, G., Francois, B. and Malarange, G., 2012. Dynamic frequency control support by energy storage to reduce the impact of wind and solar generation on isolated power system's inertia. *IEEE Transactions on sustainable energy*, 3(4), pp.931-939.
7. Ortiga A, Milano F. Generalized model of VSC-based energy storage systems for transient stability analysis. *IEEE transactions on Power Systems*. 2015 Nov 20;31(5):3369-80.
8. Inthamoussou FA, Pegueroles-Queralt J, Bianchi FD. Control of a supercapacitor energy storage system for microgrid applications. *IEEE transactions on energy conversion*. 2013 Sep;28(3):690-7.
9. Wu, J., Wen, J., Sun, H. and Cheng, S., 2012. Feasibility study of segmenting large power system interconnections with AC link using energy storage technology. *IEEE Transactions on Power Systems*, 27(3), pp.1245-1252.
10. Fang, J., Yao, W., Chen, Z., Wen, J. and Cheng, S., 2013. Design of anti-windup compensator for energy storage-based damping controller to enhance power system stability. *IEEE Transactions on Power Systems*, 29(3), pp.1175-1185.
11. Jankovic, Z., Novakovic, B., Bhavaraju, V. and Nasiri, A., 2014, September. Average modeling of a three-phase inverter for integration in a microgrid. In *2014 IEEE Energy Conversion Congress and Exposition (ECCE)* (pp. 793-799). IEEE.
12. Choi JW, Sul SK. Inverter output voltage synthesis using novel dead time compensation. *IEEE transactions on Power Electronics*. 1996 Mar;11(2):221-7.
13. Tremblay, O., Dessaint, L.A. and Dekkiche, A.I., 2007, September. A generic battery model for the dynamic simulation of hybrid electric vehicles. In *2007 IEEE Vehicle Power and Propulsion Conference* (pp. 284-289). Ieee.
14. Koenig S, Muller P, Leibfried T. Design and comparison of three different possibilities to connect a vanadium-redox-flow-battery to a wind power plant. In *Proc. 13th CHLIE 2013 Jul* (pp. 1-8).
15. Ashabani, S.M. and Mohamed, Y.A.R.I., 2014. New family of microgrid control and management strategies in smart distribution grids—analysis, comparison and testing. *IEEE Transactions on Power Systems*, 29(5), pp.2257-2269.
16. Liserre M, Blaabjerg F, Hansen S. Design and control of an LCL-filter-based three-phase active rectifier. *IEEE Transactions on industry applications*. 2005 Sep 1;41(5):1281.